Technical University of Denmark

DTU

Predicting the Influence of Surface Protuberance on the Aerodynamic Characteristics of a NACA 633-418
Paper

Krog Kruse, Emil; Sørensen, Niels N.; Bak, Christian

DTU Library
Technical Information Center of Denmark

Predicting the Influence of Surface Protuberance on the Aerodynamic Characteristics of a NACA 63_3-418

View the article online for updates and enhancements.

Related content

- Computational analysis of aerodynamic characteristics for wing in ground effect craft in lateral stability
M A U Amir, A Maimun, S Mat et al.

- Spin-dependent transport in armchair graphene nanoribbon structures with edge roughness effects
V Hung Nguyen, V Nam Do, A Bournel et al.

- The Effect of Mounting Vortex Generators on the DTU 10MW Reference Wind Turbine Blade
Witold Skrzypiski, Mac Gaunaa and Christian Bak

Predicting the Influence of Surface Protuberance on the Aerodynamic Characteristics of a NACA 63₃-418

Emil Krog Kruse[1,2], Niels N. Sørensen[2] and Christian Bak[2]

[1]Power Curve ApS, Stationsmestervej 81, DK-9200 Aalborg SV, Denmark
[2]Technical University of Denmark, Department of Wind Energy, Frederiksborgvej 399, DK-4000 Roskilde, Denmark

E-mail: `eko@powercurve.dk`

Abstract. Leading Edge Roughness (LER) has become a critical challenge for wind turbine operators, often reducing the energy production of their turbines. LER has not yet been systematically categorized, and the transfer function between height/extent of roughness and the aerodynamic performance has not been established. A common method for emulating LER is to use zigzag tape or distributed sand grain roughness in a wind tunnel. This paper contains 2D and 3D CFD simulations and wind tunnel tests with zigzag tape on a NACA 63₃-418 airfoil, to evaluate the changes in aerodynamic characteristics. Because 3D CFD requires a vast amount of computing power, it is investigated if 2D simulation gives a sufficient level of accuracy.

1. Introduction

It is known that the flow behavior of a fluid is influenced by the shape and the conditions of the surfaces nearby where the fluid passes [1]. In aerodynamics, a rough surface is known to have a negative impact on the boundary layer properties resulting in a higher drag, and for airfoils also a decrease in lift. Wind turbine blades are known to suffer from contamination in the form of bugs, moss and dirt in general[2, 3]. Wear and tear of the wind turbine blades over time can also result in erosion that gives the surface a certain roughness height. These different disturbances are generally described as Leading Edge Roughness (LER). From experience, the LER often causes a 1-7% loss in annual energy production (AEP), but it can cause as high as 20% (estimated by PROPID based on Wind Tunnel Tests, see [4]) for some airfoil families in severe cases [5–7]. The loss in AEP dealt with in this paper is less severe.

Cleaning or repairing of wind turbine blades is difficult and expensive compared to airplane wings, due to their location and accessability, thus the loss in power has to be high before measures are taken by the turbine owner. The critical height of roughness scales proportionally with rotor diameter between $R^{0.5}$ and $R^{0.8}$ [8], i.e. larger blades generally suffer relatively more from the presence of LER than smaller blades, given the LER has the same relative size to the blade. This makes the prediction of aerodynamic changes due to LER important for wind turbines.

In the past, a series of devices attached to airfoil surfaces, known in the literature as protuberances, have been used to emulate LER, mainly in wind tunnel tests. [9] This includes stall strips, trip strips and zigzag (ZZ) tape. The devices all serve the same purpose: To trip the flow and provoke a premature turbulent boundary layer and possibly separation of the

flow. Descriptions of simulations of such protuberances have not been found by the authors. Simulations on airfoils with ice accretion have been made, but the extent of ice on airfoils is much higher than the described LER and mostly conducted for airplanes with higher mach numbers than wind turbines, see [10–17]. Some simulations have also been conducted on sandpaper as LER using roughness models for simulations, see [18, 19]. The present studies are the reasons for this investigation.

The computational code used to predict the aerodynamic characteristics of a common NACA 63_3-418 is the Danish Technical University (DTU) Wind Energy in-house Computational Fluid Dynamic (CFD) software Ellipsys2D and Ellipsys3D. The NACA 63_3-418 airfoil is well known and has previously been simulated in Ellipsys2D [20–22]. The objective of this paper is to investigate the possibility of simulating the flow on the NACA 63_3-418 with protuberances modeled in the grid in 2D and predict the aerodynamic characteristics.

2. Methods
This section describes the experiments with protuberances in the form of wind tunnel tests and general CFD setup.

2.1. Experiments
A series of experiments have been conducted in the Laminar Wind Tunnel (LWT) at the Institute for Aerodynamics and Gas Dynamics, University of Stuttgart, in 2015. [23] The Stuttgart LWT has a test section of 0.73 m x 2.73 m with a length of 3.15 m. Lift was determined by integration of pressure distribution along the tunnel walls, and drag was determined by an integrating wake rake. The chord c of the NACA 63_3-418 test airfoil was 600 mm. The experiments used in this article are all conducted at a Reynolds number of Re = 3 million. The test section can be seen in Figure 1.
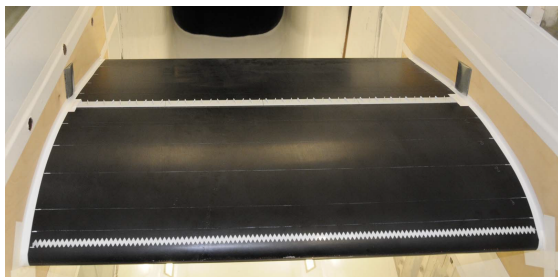
Figure 1. Wind turbine blade model in Stuttgart LWT seen with ZZ tape on the leading edge and Vortex Generators around x/c = 0.5 suction side.
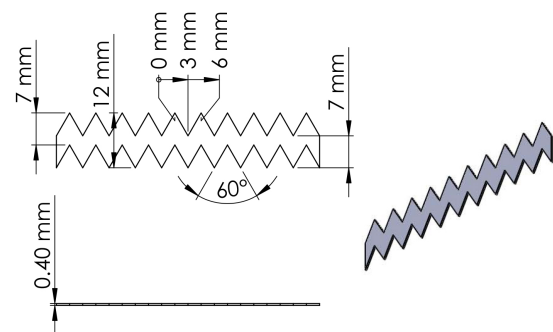
Figure 2. Dimensions of the ZZ tape used as LER in the experimental setup. Two pieces were put on top of each other to give the ZZ tape height of 0.8 mm.

To emulate LER, the wind turbine blade model is equipped with ZZ tape at x/c = 0.02 suction side and x/c = 0.1 pressure side. The zigzag (ZZ) tape has a height of 0.4 mm and measures 7 mm in width as illustrated in Figure 2.

2.2. Simulations
The simulations are based on the same notations as the wind tunnel tests. In text and figures, the different results will be presented with the following notation: Wind tunnel test results is "WT". Simulated results are denoted "CFD". Cases with no LER is "Clean", the 0.4 mm ZZ

tape is "0.4", and the 0.8 mm ZZ tape is "0.8". Likewise, it will be noted if it is 2D or 3D simulations. The 0.8 mm ZZ tape is obtained by using two 0.4 mm strips layered on top of each other.

2.2.1. Grid   The grid is constructed using the geometry of the measured airfoil from the wind tunnel test. Some deviation between the theoretical and measured NACA 63_3-418 test airfoil was evident, especially at the leading edge. It was chosen to simulate on the measured airfoil to get the most accurate results. Smoothing was applied to the measured points within reasonable limits. It is constructed using the DTU Wind in-house HypGrid2D, a 2-D Mesh Generator [24]. An overview of combinations and notations are given in table 2.2.1:

Notation	Description
s.s.	Suction Side of the airfoil
p.s.	Pressure Side of the airfoil
Clean 2D	NACA 63_3418 2D simulations without protuberance ("Clean")
Clean 3D	NACA 63_3418 3D simulations without protuberance ("Clean")
0.4 mm 2D	0.4 mm zigzag tape in 2%c s.s. and 10%c p.s. in 2D simulation
0.6 mm 2D	0.6 mm zigzag tape in 2%c s.s. and 10%c p.s. in 2D simulation
0.8 mm 2D	0.8 mm zigzag tape in 2%c s.s. and 10%c p.s. in 2D simulation
0.4 mm pseudo 2D	0.4 mm 2D extruded spanwise and simulated in 3D
0.6 mm pseudo 2D	0.6 mm 2D extruded spanwise and simulated in 3D
0.8 mm pseudo 2D	0.8 mm 2D extruded spanwise and simulated in 3D
0.4 mm 3D	0.4 mm zigzag tape in 2%c s.s. and 10%c p.s. in 3D simulation
0.6 mm 3D	0.6 mm zigzag tape in 2%c s.s. and 10%c p.s. in 3D simulation
0.8 mm 3D	0.8 mm zigzag tape in 2%c s.s. and 10%c p.s. in 3D simulation
WT	WT is noted for coefficients measured in a Wind Tunnel
CFD	CFD is noted for CFD simulated coefficients
Grid-A	Profile grid used in 2D simulations, 0.4, 0.6 or 0.8 mm zigzag tape
Grid-B	Profile grid used with grid-A to form a 3D grid

The grid of the clean airfoil can be seen in Figure 3. A structured O-mesh with a domain radius of 45 times the chord has been used. The simulated airfoil chord is 1 m.

The zigzag tape height and width is scaled accordingly with 1000mm/600mm. Figure 3 shows the total 2D grid domain of the clean airfoil. Figure 4 shows a close up of the grid of the clean airfoil. Only every 4th grid line is shown. The total number of cells in the circumferential direction is 512 and 384 in the normal direction, a total of 196,608 cells in the 2D grids. The high number of cells was necessary to get grid-independent results in 3D simulations with the 0.8 mm ZZ protuberance, described in section 3. The boundary layer consist of approximately 60 cells where the boundary layer is thinnest, which also applies for the boundary layer on top of the ZZ tape. All wall cells on the airfoil are $\approx 1 \cdot 10^{-6}$ chord length, which results in a y+ of 0.1-0.2 for all wall cells. To achieve uniformity, the same grid settings were used for all simulations. The outlet is around 45° and can be seen together with the grid blocks in Figure 5. The grid blocks make it possible to run on multiple CPU's [24].
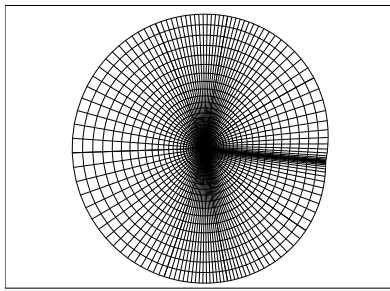
Figure 3. Grid lines in the total domain, shown is coarser level 3 grid
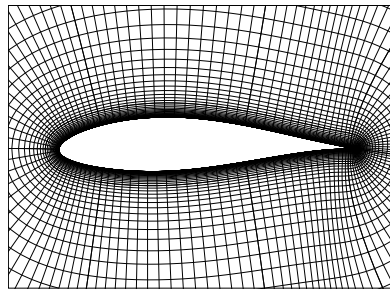

**Figure 4.** Grid lines around the airfoil, shown is coarser level 3 grid
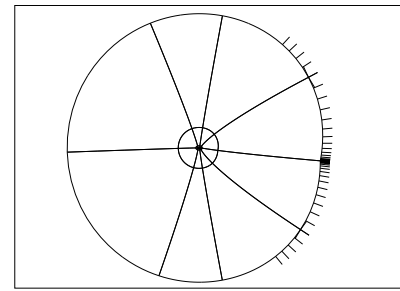
Figure 5. Grid blocks with inlet and outlet, shown is coarser level 3 grid

The grid used for 3D simulations has the same amount of cells and cell distribution as in 2D. The 3D grid is made from two grids, grid-A and grid-B. Grid-A is identical to the corresponding 2D grids, whereas grid-B has the ZZ tape shifted towards the trailing edge, see Figure 7. Naturally, there is a grid-A and grid-B for both 0.4, 0.6 and 0.8 mm ZZ tape and the clean airfoil. The spanwise length is 0.02 m. The unscaled ZZ tape has a tip-to-tip distance of 6 mm, which results in 10 mm when scaled by 1000mm/600mm, hence the 0.02 m span contains two periods of ZZ tape form as depicted in Figure 6-8. It could be limited to a span of 0.01 m, but for illustration purposes it was chosen to use 0.02 m. Each of the two ZZ tape instances is divided into 8 cells each with the same spanwise length, resulting in a total of 32 cells in the spanwise direction, resulting in a total of 6,291,456 cells in the 3D cases. The ZZ tape height was also simulated with 12 and 16 cells, but gave results similar to 8 cells. A periodic condition is applied to the spanwise boundaries. Grid-A blends into grid-B in the farfield using a tanh function over the first 150 cells, resulting in stable 3D simulations. All coefficients calculated for 3D cases are spanwise averages.
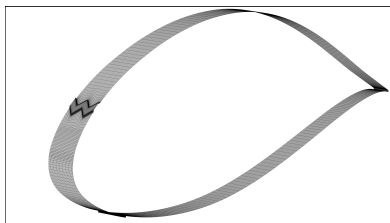
Figure 6. Perspective view of ZZ on airfoil. The entire span wise domain is shown
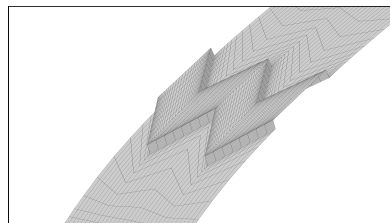
Figure 7. Closeup of ZZ tape grid. The entire span wise domain is shown
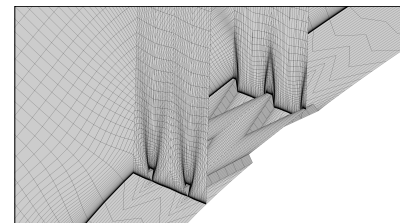
Figure 8. Closeup of ZZ tape grid with three planes showing the grid normal to the airfoil

2.2.2. Numerical Setup One goal of the project was to investigate if the in-house DTU CFD software EllipSys was capable of simulating protuberances or if optimisation was needed. EllipSys is an incompressible finite volume RANS flow solver, which uses the SIMPLE algorithm to solve the Navier-Stokes equations [25–28]. The QUICK scheme is used to discretize the convective terms, see [29]. A relaxation of 0.6 is used on all velocities, and a relaxation of 0.1 on the pressure in all simulations. The density of the fluid is 1 kg/m^3, the chord is 1 m, and the dynamic viscosity is $3.333 \cdot 10^{-7}$ m^2/s. The inlet is laminar flow with a velocity of $[u; v; w] = [1; 0; 0]$ m/s for an Angle of Attack (AoA) of 0 deg. These inputs result in a Reynolds number

of 3 mio. All simulations run untill convergence with the limit of $1 \cdot 10^{-6}$ of the error in the first iteration.

Menter's k-ω with SST is used as turbulence model [30]. The e^N by Drela-Giles is used to simulate transition and separation of the flow. [31] The N factor was tested with values from 3 to 9 with an increment of 1 and found to give the best fit with N = 9 in the clean case, hence this factor is used in all simulations. The calibration of the N factor was mainly based on lift and drag fits between the experimental results and the CFD simulations for the clean situation.

The simulations are done on coarser level 2 and 3 to assure grid-independent results. All simulations are run from -5 to 12 deg AoA as no steady solution was found in the 3D simulations above 12 deg AoA. Furthermore, no wind tunnel drag measurements are present above 10 deg AoA.

3. Results and Discussion

A first glance at the simulation results in Figure 9 for the clean airfoil shows good correspondence between grid levels. A reduction in cells causes changes in lift and drag for AoA above 9 deg. The results are in close agreement and the grid resolution is acceptable.
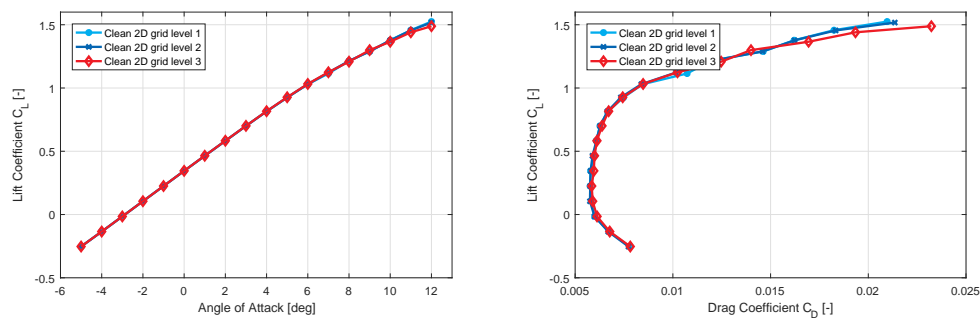
Figure 9. Comparison of Coarser grid level 1, 2 and 3 lift and lift/drag

3.1. Wind Tunnel vs. CFD: Clean Airfoil

The next natural step is to compare the clean simulations for both 2D and 3D simulations to the WT Clean results. The 3D grid is constructed using the same grid file in each spanwise position. The results can be seen in Figure 10.
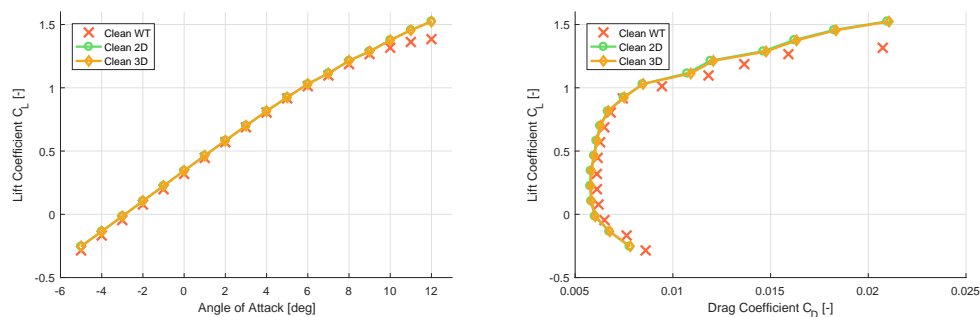
Figure 10. Comparison of Clean 2D, Clean 3D and Clean Wind Tunnel test results lift and lift/drag

The 2D and 3D results are similar. The drag is slightly higher in 3D, probably from the cross flows induced by the turbulence model, which has been examined in streamline plots, although

the cross flows are small. The WT Clean test data is slightly lower in lift for negative AoA. Stall is not predicted to be as severe in simulations as in the WT test. There will be differences between the implementation methods of the simulation models in 2D and 3D. The lift/drag ratio correspondence is as good as can be expected.
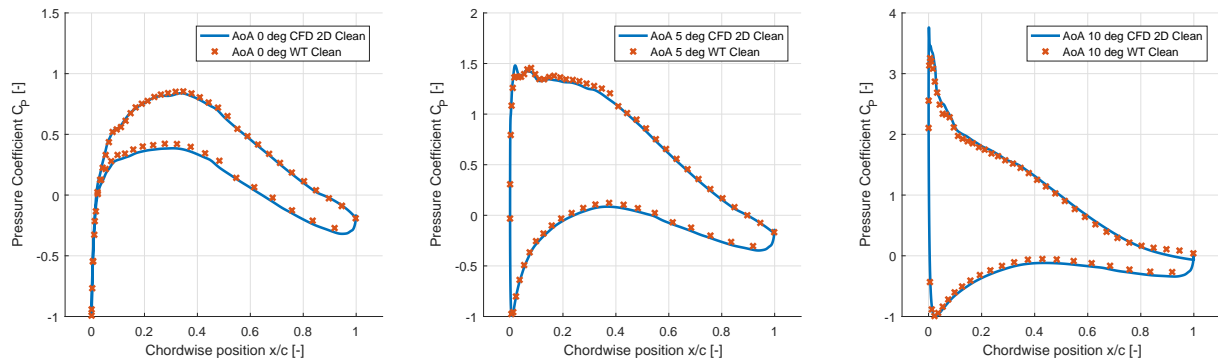

Figure 11. Pressure coefficients C_P for CFD simulation and wind tunnel tests for 0, 5 and 10 deg AoA.

A comparison of the pressure coefficients (C_P) is done at 0, 5 and 10 deg AoA. Figure 11 shows the 2D CFD Clean against the WT Clean test. In all cases the pressure is predicted to be slightly lower than measurements, which might explain the small deviation in drag. No tunnel correction has been applied to the measured C_P which will introduce some deviation between simulation and test data.

3.2. Wind Tunnel vs. CFD: Protuberance Airfoil

As partly described in section 2.2.1, the grid is made in both 2D and 3D. An intermediate step has been introduced, which is called "pseudo-2D". In this step grid-A is used also as grid-B, to see the effect of 2D LER in 3D. This is done because zigzag tape cannot be modeled in 2D CFD. Here it turns into a bump with no geometrical changes in the spanwise direction.
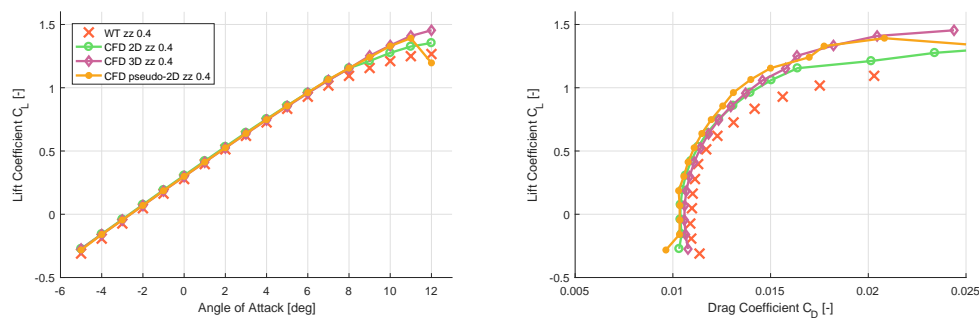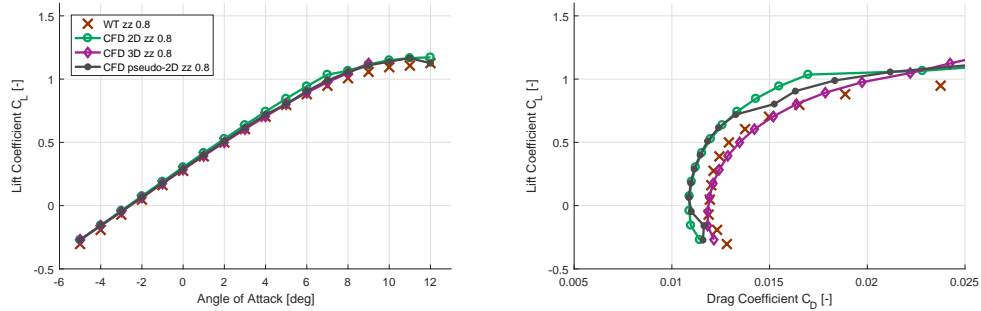

Figure 12. Comparison of lift and lift/drag for simulations and WT test with 0.4 mm ZZ tape

Figure 12 shows the simulated and measured lift as a function of AoA (left) and as a function of drag (right) for the 0.4 mm ZZ tape case. As in the clean case, the 3D computations predict the drag better at low AoA. The lift is still over-predicted, especially in the stall region. Figure 13 shows the simulated and measured lift and lift/drag for the 0.8 mm ZZ tape case.

A difference between 2D and 3D can be seen, with a much higher drag and better correspondence in the 3D case. The pseudo-2D simulations predict the flow just as 2D from -5 to 4 deg AoA and slightly better above that, but not as well as the real 3D simulation.
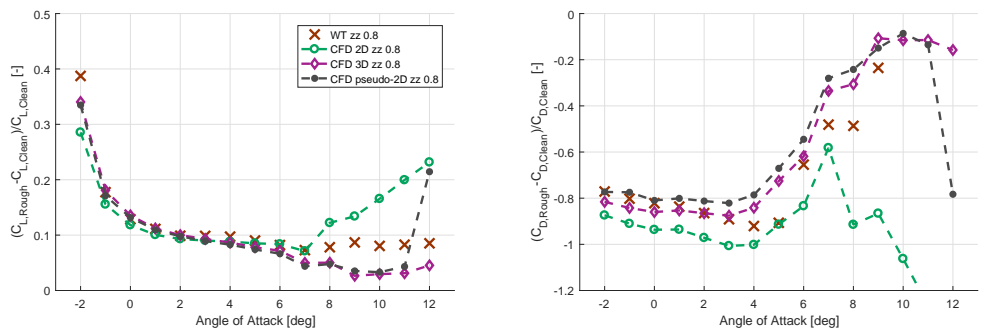
Figure 13. Comparison of lift and lift/drag for simulations and WT test with 0.8 mm ZZ tape

It can be difficult to see how well the simulation predicts the WT tests solely from lift and drag values. A relation between the Clean and ZZ tape cases is introduced as $(X_{Clean} - X_{Rough})/X_{Clean}$ where X is C_L or C_L/C_D for either CFD or WT test. The ratios are plotted in Figure 14 and 15. The best-case correspondence is a CFD ratio equal to the WT ratio.
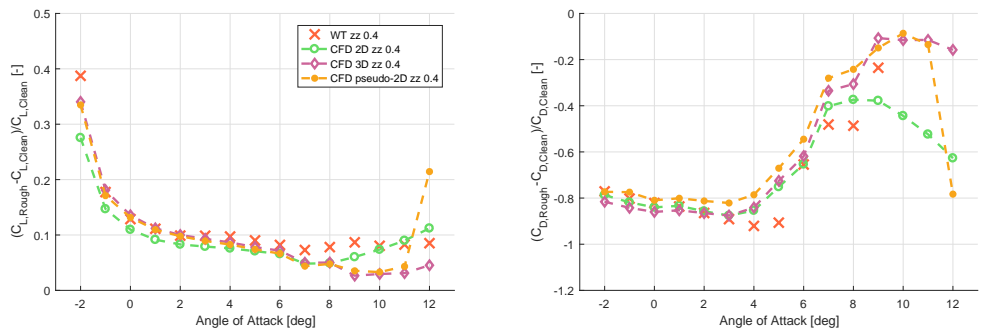
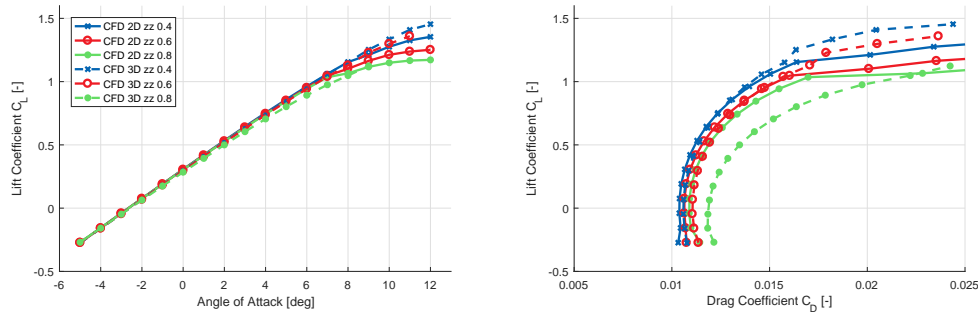**Figure 14.** Comparison of lift and lift/drag ratios for simulations and WT test with 0.4 mm ZZ tape

Figure 15. Comparison of lift and lift/drag ratios for simulations and WT test with 0.8 mm ZZ tape

From Figure 14 and 15 it is easier to see that the simulations show high deviation from 7 deg AoA and up. The best match is still 3D, even though the deviation at AoA above 7 deg increases, but the trends remain.

A relation between 2D and 3D simulation with ZZ tape is difficult to establish based on two cases. Therefore, a third case is introduced, being 0.6 mm ZZ tape. However, no WT tests are available for this. Based on the results described above, it is concluded that EllipSys2D and EllipSys3D are both capable of simulating this kind of geometry, and the 0.6 mm case relies solely on the CFD simulations. The simulation results for Clean, 0.4, 0.6 and 0.8 mm ZZ tape are collected in Figure 16.

Figure 16. Comparison of lift and lift/drag ratios for simulations and WT test with 0.8 mm ZZ tape

From Figure 16, a linear relation between ZZ tape height and drag coefficient C_D in 2D is observed. The 3D simulations have a non-linear relation. It would be possible to estimate a correction factor when going from 2D to 3D, but the data basis for this is not present. There are too many unknown parameters such as the chord-wise location of the protuberance, the angle in the protuberance (being 60 deg here), edge angles on the protuberance and the fact that the shape will never be as clearly defined and periodic in real LER cases. In the case of 60 deg ZZ tape, the third dimension of the ZZ tape has very little impact on 0.4 mm, medium impact on 0.6 mm and quite a high impact on 0.8 mm.
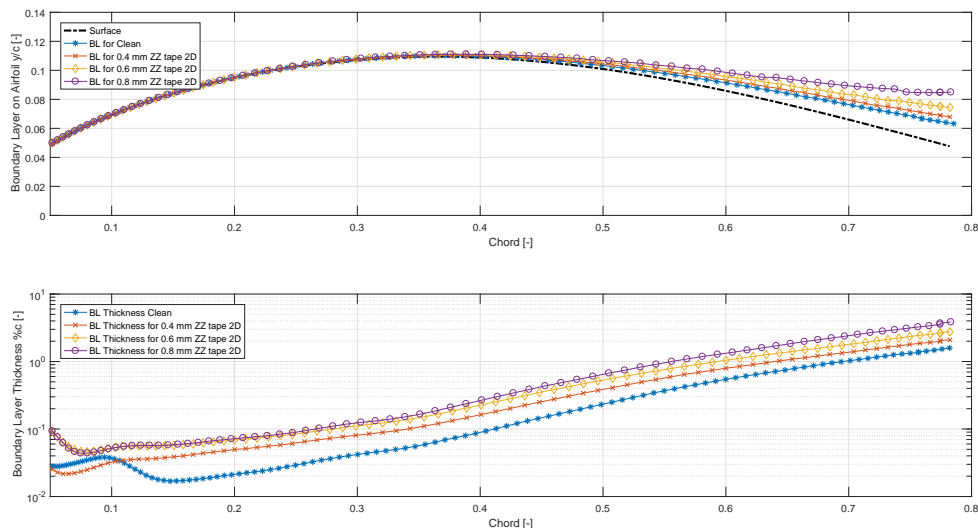
Figure 17. Quantitative comparison of the boundary layer for 2D situations with Clean from both CFD, 0.4 mm, 0.6 mm and 0.8 mm ZZ tape for AoA 8 deg.

Figure 17 shows the boundary layer of the s.s. for 2D simulations of 0.4, 0.6 and 0.8 mm ZZ tape compared to the clean airfoil in AoA 8 deg. The boundary layer is found to be in cells where the absolute velocity is 99% of the free stream velocity. The upper figure shows the airfoil surface and the boundary layer. It is clear that higher ZZ tape results in a thicker boundary layer, leading to earlier separation of flow. The lower figure shows the height of the boundary layer on a Y log scale. Again, the boundary layer thickness is thicker for higher ZZ tape, especially after 0.5 chord length.
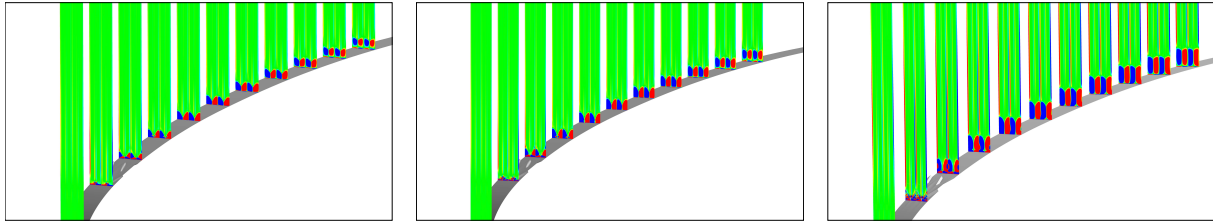
Figure 18. Vorticities for 0.4 mm 3D ZZ tape

Figure 19. Vorticities for 0.6 mm 3D ZZ tape

Figure 20. Vorticities for 0.8 mm 3D ZZ tape

Figure 18-20 show the vorticities in the flow along the airfoil. The colorbar is set to be from -5 to 5 for all three ZZ heights. It is clear how the cases with 0.6 and 0.8 mm ZZ tape are subjected to stronger vorticities both close to the airfoil and in the normal direction. The 3D effect in the 0.4 mm ZZ case is present but low. It can also be seen that double ZZ tape height results in more than double the vorticity size.

One of the conclusions of the investigations above is that 2D simulations can be used to predict the flow for a 3D situation up until a certain height of the protuberance. Since the computational time is longer compared to 2D and the complexity of making the grid for 3D is much higher, the accuracy is deemed acceptable for 2D simulations.

4. Conclusion

As stated in section 1, existing literature deals with the simulations of LER as being either ice accretion, simulated by implementing the ice structure directly in the grid or smaller LER like sandpaper or particles simulated by a roughness model. The possibility of simulating small LER with a size (height or depth) of 0.1%c and above, has been investigated in this paper.

Both EllipSys2D and EllipSys3D are able to predict the transient solution for the angles in the range -5 to 12 deg AoA. EllipSys3D struggles with solutions for steady simulations in the range from 9 to 12 deg AoA when the protuberance/LER becomes larger than approximately 1%c. For the EllipSys2D simulations no such problems are experienced. Simulations have been compared to wind tunnel tests and generally good agreement is found. As often seen, the maximum lift is over predicted simulations as well as an underrated drag. Differences between 2D and 3D simulations is found where the drag in particular is predicted better in 3D, however, the significantly lower calculation time and grid complexity justifies simulations done in 2D.

The final conclusion states that it is indeed possible to simulate small LER by direct implementation in the grid, and it is to some extent sufficient to do simulations in 2D rather than 3D.

References

[1] Hoerner S F 1965 *Fluid-Dynamic Drag* (USA) Hoerner

[2] Corten G P and Veldkamp H F 2001 *Aerodynamics: Insects can halve wind-turbine power* vol 412, 4142

[3] Bak C, Andersen P B, Madsen H A, Gaunaa M, Fuglsang P and Bove S 2008 *Design and verification of airfoils resistant to surface contamination and turbulence intensity* vol AIAA 2008-7050 (Reston, VA (US)) American Institute of Aeronautics & Astronautics

[4] Sareen A, Sapre C A and Selig M S 2014 *Effects of leading edge erosion on wind turbine blade performance* Department of Aerospace Engineering, University of Illinois at Urbana-Champaign, Urbana, IL 61801, USA

[5] van Rooij R and Timmer W A 2003 *Roughness Sensitivity Considerations for Thick Rotor Blade Airfoils* vol 125

[6] Hooker R W 1933 *The aerodynamic characteristics of airfoils as affected by surface roughness* (Washington) NACA-TN-457 Langley Memorial Aeronautical Laboratory

[7] Gaudern N 2014 *A practical study of the aerodynamic impact of wind turbine blade leading edge erosion* Vestas Technology UK Ltd.

[8] Bak C, Gaunaa M, Olsen A S and Kruse E K 2016 *What is the critical height of leading edge roughness for aerodynamics?* vol 753

[9] Bak C, Fuglsang P, Johansen J and Antoniou I 2000 *Wind Tunnel Tests of the NACA 63-415 and a Modified NACA 63-415 Airfoil* (Risø National Laboratory)

[10] Bragg M, Broeren A, Addy H, Potapczuk M, Guffond D and Montreuil E 2007 *Airfoil ice-accretion aerodynamic simulation*

[11] Sermeus K and Yang H 2015 *CFD Simulation of Aircraft Icing Effects using Roughness Modeling*

[12] Broeren A P, Addy H E, Bragg M B, Busch G T, Guffond D and Montreuil E 2011 *Aerodynamic Simulation of Ice Accretion on Airfoils* NASA

[13] Cebeci T 1987 *Effect of Intercycle Ice Accretions on Airfoil Performance* California State University (NASA)

[14] Broeren A P, Bragg M B and Addy H E 2004 *Effects of Environmentally Imposed Roughness on Airfoil Performance*

[15] Turkia V, Huttunen S and Wallenius T 2013 *Method for estimating wind turbine production losses due to icing* VTT Technology)

[16] Mortensen K 2008 *CFD simulations of an airfoil with leading edge ice accretion* Technical university of Denmark

[17] Langel C M, Chow R, Hurley O F, van Dam C P, Ehrmann R S and White E B 2015 *Analysis of the Impact of Leading Edge Surface Degradation on Wind Turbine Performance* AIAA

[18] Standish K, Rimmington P, Laursen J and Paulsen H N 2010 *Computational Prediction of Airfoil Roughness Sensitivity*

[19] Ehrmann R S, White E B, Maniaci D C, Chow R, Langel C M and van Dam C P 2013 *Realistic Leading-Edge Roughness Effects on Airfoil Performance*

[20] Bertagnolio F, Sørensen N, Johansen J and Fuglsang P 2001 *Wind Turbine Airfoil Catalogue* (DK-4000 Roskilde) Risø National Laboratory

[21] White E B, Kutz D, Freels J, Hidore J P, Grife R, Sun Y and Chao D 2011 *Leading-Edge Roughness Effects on 63₃-418 Airfoil Performance*

[22] Timmer W A 2009 *An Overview of NACA 6-Digit Airfoil Series Characteristics with Reference to Airfoils for Large Wind Turbine Blades*

[23] Würz W and C Vetter M L K 2015 *Wind Tunnel Measurements of the NACA 63₃-418 Airfoil with Vortex Generators (Confidential)* IAG, Universität Stuttgart

[24] Sørensen N 1998 *HypGrid2D, a 2-D Mest Generator* Risø National Laboratory

[25] Ceyhan O, , Pires O, Munduate X, Sorensen N N, Schaffarczyk A P, Reichstein T, Diakakis K, Papadakis G, Daniele E and Schwarz M 2017 *Summary of the Blind Test Campaign to predict the High Reynolds number performance of DU00-W-210 airfoil*

[26] Michelsen J 1992 *Basis3D - a Platform for Development of Multiblock PDE Solvers*

[27] Michelsen J 1994 *Block structured Multigrid solution of 2D and 3D elliptic PDE's*

[28] Sørensen N 1995 *General Purpose Flow Solver Applied to Flow over Hills* Risø National Laboratory

[29] Leonard B P 1979 *A stable and accurate convective modelling procedure based on quadratic upstream interpolation* Comput. Meths. Appl. Mech. Eng

[30] Menter F R 1993 *Zonal Two Equation k-omega Turbulence Models for Aerodynamic Flows*

[31] Drela M and Giles M B 1987 *Viscous-Inviscid Analysis of Transonic and Low Reynolds Number Airfoils*